Hawke’s Bay 3D Aquifer Mapping Project:

Hydrostratigraphic modelling in the Ruataniwha Plains

November 2023
Hawkes Bay Regional Council Publication No. 5629

HAWKES BAY
REGIONAL COUNCIL
TE KAUNIHERA Ā-ROHE O TE MATAU-A-MĀUI

ISSN 2703-2051 (Online)
ISSN 2703-2043 (Print)

(06) 835 9200
0800 108 838
Private Bag 6006 Napier 4142
159 Dalton Street . Napier 4110

Environmental Science

Hawke’s Bay 3D Aquifer Mapping Project:

Hydrostratigraphic modelling in the Ruataniwha Plains

November 2023
Hawkes Bay Regional Council Publication No. 5629

Prepared By:

GNS Science

M Herpe ZJ Rawlinson

For: Hawke’s Bay Regional Council

Reviewed by:
S Harper, Hawke’s Bay Regional Council
R Reeves, GNS Science
C Tschritter, GNS Science

ISSN 2703-2051 (Online)
ISSN 2703-2043 (Print)

.

Letter Report No: CR 2023/102 LR
Project No: 900W4090-13
Confidential 2023

27 November 2023

Team Leader - Hydrology and Groundwater Science
Hawke's Bay Regional Council
159 Dalton Street
Napier 4110

Wairakei Research Centre
114 Karetoto Road
RD 4
Taupō 3384
Private Bag 2000
Taupō Mail Centre
Taupō 3352
New Zealand
T +64-7-374 8211
F +64-7-374 8199
www.gns.cri.nz

Attention: Simon Harper

Dear Simon,

Hawke's Bay 3D Aquifer Mapping Project: Hydrostratigraphic modelling in the Ruataniwha Plains

1.0 SUMMARY

As part of the Hawke's Bay 3D Aquifer Mapping Project (3DAMP), this report focuses on hydrostratigraphic modelling (HSM) in the Ruataniwha Plains area using SkyTEM-derived resistivity models combined with a classified and quality-coded lithological dataset.

The HSM-concept provides a framework to develop spatially-varying relationships between resistivity and permeability within the unconsolidated sediments of the Ruataniwha Plains. The HSM-concept has been implemented through four distinct steps: (1) selection of SkyTEM-derived resistivity models corresponding to unconsolidated sediments; (2) a permeability classification of the lithological logs; (3) Accumulated Clay Fraction (ACT) modelling; and (4) a k-means clustering routine. At locations of SkyTEM-derived resistivity models, this framework translated the resistivity models into six hydrostratigraphic units, ranging from the most clay-rich unit (aquitard with >70% clay) to the most permeable unit (aquifer with <10% clay). Measures of uncertainty are provided by the clay fraction standard deviation and the clustering silhouette index.

The results will be utilised within subsequent modelling work as part of 3DAMP.

2.0 INTRODUCTION AND INPUT DATA

This report derives a hydrostratigraphic model of the unconsolidated sediments of the Ruataniwha Plains using SkyTEM data (SkyTEM Australia Pty Ltd. 2020 and Rawlinson et al. 2022) and other supporting information. This work was undertaken as part of the 3DAMP.

3DAMP is a four-year initiative (2019–2023) jointly funded by the Provincial Growth Fund (PGF), Hawke's Bay Regional Council (HBRC), and GNS Science's Groundwater Strategic Science Investment Fund (SSIF) research programme.

A thorough review of the geology, hydrogeology, available data, and previous-developed hydrogeological models in the Ruataniwha Plains model area (Figure 2.1) has been provided in Tschritter et al. (2022). The primary datasets utilised for the hydrostratigraphic model include:

1. A SkyTEM-derived sharp resistivity model (Figure 2.1; Rawlinson et al. 2022).
2. A quality-coded lithological log dataset (Figure 2.2; Tschritter et al. 2022).
3. A hydrogeological basement interpretation surface (Sahoo et al. 2023).

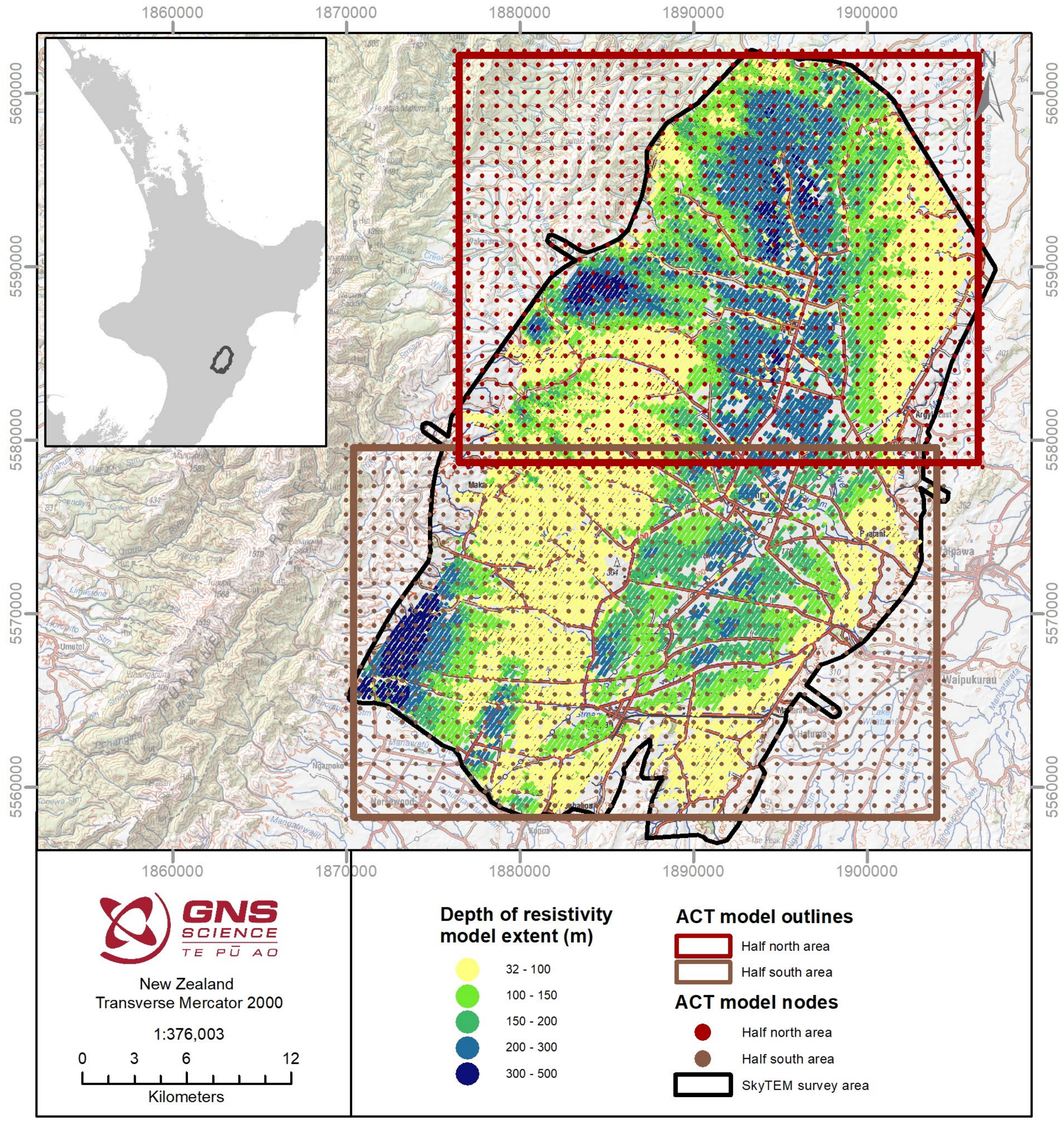

Figure 2.1 Location map of the Ruataniwha Plains showing the depth and extent of the resistivity models used in the HSM, as well as the ACT model nodes and grid extents. See Section 3.0 for further details.

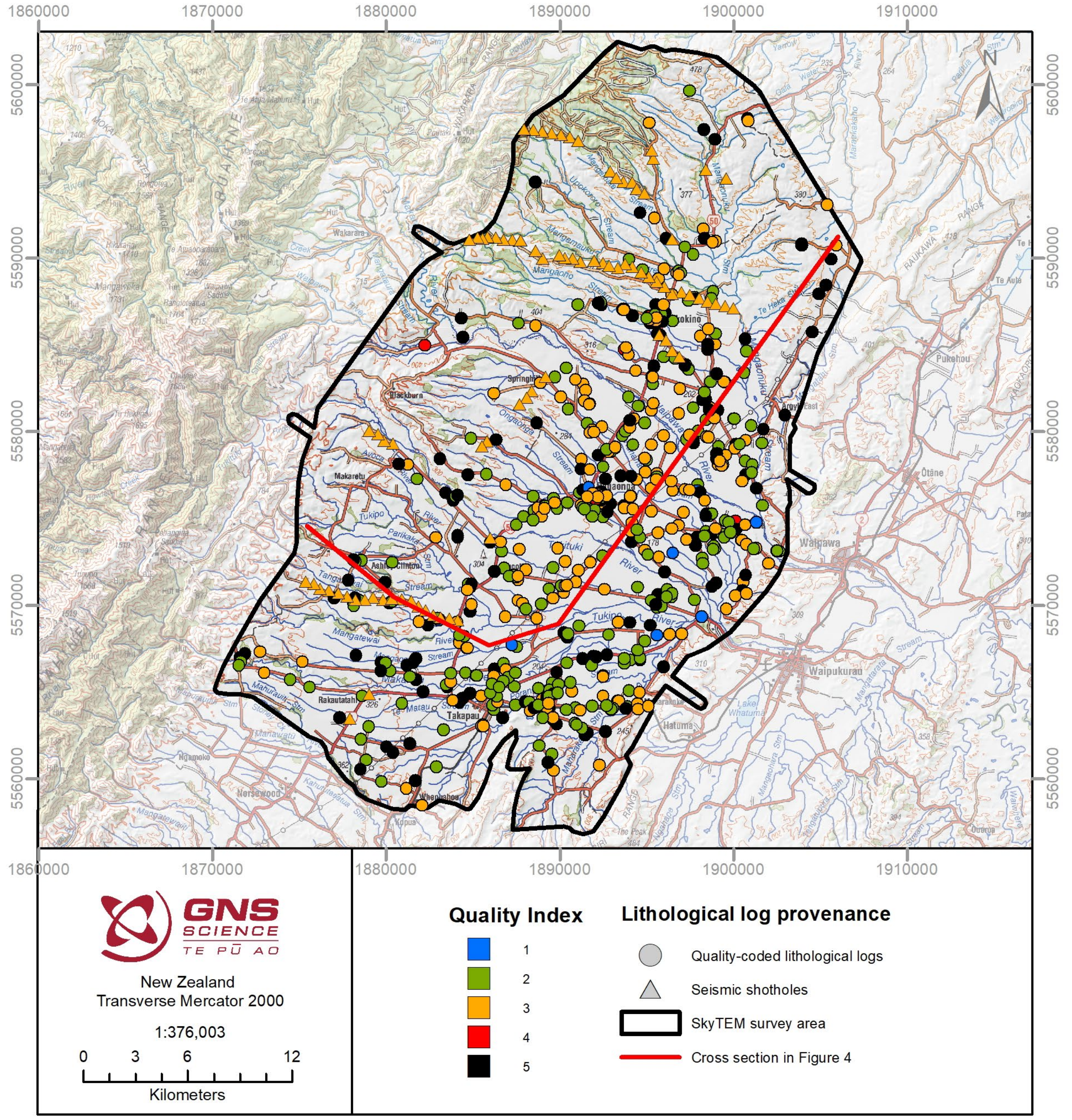

Figure 2.2 Location map of the borehole dataset used in the HSM. The borehole marker shape corresponds to the provenance of the datasets, while the borehole marker colour corresponds to the assigned quality index (1 is the highest quality and 5 the lowest). The lithological logs from the seismic shotholes were attributed a quality index of 3. The boreholes with a quality index of 5 (in black) were filtered out in the study. The location of the cross-section (E–NW) in Figure 4.1 is shown by the red line. See Section 3.0 for further details.

3.0 METHOD

3.1 HydroStratigraphic Modelling (HSM)

This section presents a short, general description of the HSM-concept implemented in this report. A more detailed explanation of the methodology is available in Foged (2022), Christiansen et al. (2014), Foged et al. (2014), Marker et al. (2015) and Vilhelmsen et al. (2019).

The HSM-concept provides a framework to estimate permeability at resistivity model locations. The method estimates spatially-varying relationships between resistivity and permeability, utilising lithological logs classified into permeability classes.

In this report, the HSM-concept (Figure 3.1; Marker et al. 2015) has been implemented using the HSM module of Aarhus Workbench software version 6.8.0.0. At the time of writing this report, the HSM-concept is only implementable in Aarhus Workbench up to the clustering and final data preparation step.

The HSM-concept has been implemented with the following steps (Figure 3.1):

1. Data preparation for the ACT modelling (Sections 3.2.1 and 3.2.2).
2. ACT modelling (Section 3.3).
3. Clustering and final data preparation (Section 3.4).

Two datasets were prepared for the ACT modelling: the resistivity model was clipped at depth based on the previously estimated extent of unconsolidated sediments (Section 3.2.1), and lithological logs were classified into permeability classes based on the available lithological log descriptions (Section 3.2.2). ACT models were developed at locations of SkyTEM-derived resistivity models and borehole lithological information using mathematical inversion (minimising the difference between the clay contents calculated from the resistivity models and the observed clay contents in the lithological well logs). The ACT modelling was undertaken as an iterative process between modifying the lithological log permeability classification and running the inversion to obtain a best fit to data. Additional iterative testing was also undertaken on the ACT input parameters (upper and low resistivity bounds, see Section 3.3). The ACT modelling final outputs are estimates of clay fraction (CF) and associated standard deviations at all locations of the SkyTEM-derived resistivity models. K-means clustering was then carried out on the CF–resistivity data pairs to develop a number of discrete hydrostratigraphic units. The associated silhouette index at each model position was also calculated (see Section 3.4).

As in Marker et al. (2015), the HSM-concept has only been completed up to the cluster model and subsequent data preparation stage. This is in contrast to the Heretaunga HSM work (Foged 2022) that was also undertaken as part of 3DAMP. For the Ruataniwha Plains, 3D gridding and geostatistical simulations were not undertaken because of the following:

1. Assessments of the Heretaunga HSM results revealed limitations in the 10 m vertical resolution model utilised for the 500 geostatistical realisations (Rawlinson, in prep.).
2. Ruataniwha contains few SkyTEM data gaps (compared with Heretaunga Plains)
3. Preliminary testing with the Heretaunga numerical groundwater model determined that the underlying ACT and cluster models at the locations of SkyTEM-derived resistivity models were likely more suitable than the geostatistical realisations for prior parameter conditioning for numerical modelling based on current numerical modelling workflows (Hemmings et al., in prep).

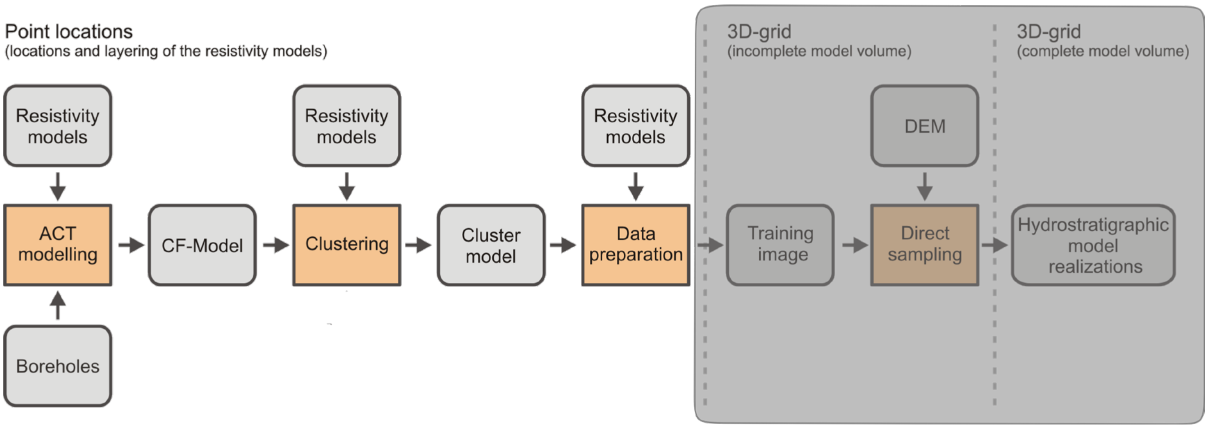

Figure 3.1 Flowchart of the HSM-concept (Foged 2022). Only the first part of the process has been completed in this report (not the greyed-out section).

3.2 Data Preparation

3.2.1 SkyTEM Data

SkyTEM data were collected over the Ruataniwha Plains in January/February 2020 by SkyTEM Australia (SkyTEM Australia Pty Ltd. 2020). From the processing of this data, both smooth and sharp resistivity models of the survey area were developed by Rawlinson et al. (2022). The sharp resistivity model was preferred over the smooth resistivity model, since the sharp model provides a sharper definition of the major resistivity structures, which is beneficial in the clustering step. These resistivity models have a Standard Depth of Investigation (DOI) calculated, below which the models become more uncertain.

The HSM-concept was developed for modelling unconsolidated sediments and relies on the assumption that a lower electrical resistivity corresponds to a lower hydrological conductivity (fine sediments, aquitard-like) and vice versa (coarse sediments, aquifer-like).

To respect this assumption, the sharp resistivity model was clipped at depth to remove the influence of consolidated sediments. Within the Aarhus Workbench implementation of this clipping, if a resistivity layer is intersected by the basement surface, it is removed. To account for this approach, and avoid loss of unconsolidated model layer information at depth, a 30 m buffer was applied to the hydrogeological basement surface delineated by Sahoo et al. (2023). The final clipping depth was set as the shallower of either the standard DOI or the hydrogeological basement surface delineated by Sahoo et al. (2023) increased by 30 m.

3.2.2 Lithological Classification

Two lithological log datasets containing a total of 756 boreholes (Figure 2.2), were utilised for the HSM:

- A quality-coded lithological log dataset containing 660 boreholes (Tschritter et al. 2022).
- Digitised lithological logs from seismic shothole data containing 96 boreholes (Tschritter et al. 2022). This dataset was attributed a quality index (QI) of 3.

Boreholes with a poor QI rating (rating of 5; Tschritter et al. 2022) were filtered out, resulting in 576 boreholes used for the HSM.

The HSM-concept requires a binary approach to the input log data classification. The lithological logs must be classified as ’Aquifer’ (most permeable material/coarse sediments) or ‘Aquitard’ (clay-rich sediments/least permeable material). Any ‘unknown’ classification enters the HSM-concept as ‘no data’.

As described in Tschritter et al. (2022), previous hydrogeological studies have identified the structural and geological complexity of the multi-layered Ruataniwha Plains aquifer system. The heterogeneous gravel and clay layers are a result of this structural and geological complexity.

In this study area, gravel, sand, silt and clay are the predominant lithologies characterising the heterogeneity of the deposits in the aquifer system. Each entry of the lithological log dataset was attributed a rock symbol based initially on primary lithologies. Subsequently, through specific text searches of the lithological log “full description” and “strata note”, each one of those four lithologies was sub-categorised to better model the effect of coarse- and fine-grained materials on the modelled resistivity values (Table 3.1). Iterative testing was then undertaken with classifying these categories into ‘Aquifer’, ‘Aquitard’ or ‘unknown’. The final classification used for the ACT modelling is shown in Table 3.1.

As an example, following the identification of the clay-bound gravels as a potential aquitard by PDP (1999), the gravel lithology was divided into five different sub-categories: pure gravels (GR1), gravels with fine-grained material (GR2), gravels with traces of fine-grained material (GR3), cemented or clay-bound gravels (GR4) and gravels with any other material (GR5). An iterative process between the classification of the five gravel sub-categories and running the ACT modelling was undertaken. The best data fit was found with classifying GR1 and GR5 as “Aquifer” and GR2, GR3 and GR4 as “Unknown”.

Three rock symbol categories were also generated, not only based on lithology but with added information from key strata descriptors:

- Aquitard (AQT): groups lithologies with keywords like “impermeable” or “no water”, “dry” for intervals at greater than 10 m depth (to remove water table associations).
- Aquifer (AQ): groups lithologies with keywords like “water bearing”, “free water” or “water yielding” and without clay, silt, limestone or sandstone as primary lithology.
- Conflicting (CONF): groups lithologies with conflicting keywords like “water bearing/yielding” and “clay-bound/cemented” and without clay as primary lithology.

Table 3.1 Lithology classification into aquitard, aquifer and unknown and their occurrence in the dataset. Lithologies classified as unknown enter the HSM-concept as “no-data”.

Lithology	Rock Symbol	Classification	Dataset Occurrence
Gravel, pure	GR1	Aquifer	19.7%
Aquifer	AQ	Aquifer	9.8%
Gravel, with other material	GR5	Aquifer	3.2%
Sand, pure	SA1	Aquifer	1.1%
Sand, with coarse-grained material	SA2	Aquifer	1.1%
Sand, with shell or limestone	SA3	Aquifer	0.3%
Clay, pure	CL1	Aquitard	19.5%
Clay, with other material	CL3	Aquitard	6.4%

Lithology	Rock Symbol	Classification	Dataset Occurrence
Silt, with coarse grained material	SI2	Aquitard	1.3%
Aquitard	AQT	Aquitard	0.8%
Mudstone	MS	Aquitard	0.5%
Siltstone	IS	Aquitard	0.5%
Silt, pure	SI1	Aquitard	0.0%
Gravel, with fine-grained material	GR2	Unknown	10.0%
Clay, with coarse-grained material	CL2	Unknown	5.9%
Fill/mud/topsoil/unknown	XX	Unknown	5.8%
Gravel, cemented	GR4	Unknown	5.0%
Limestone	LS	Unknown	2.0%
Ash/Pumice	AS	Unknown	1.9%
Sand, with other material	SA4	Unknown	1.4%
Sandstone	SS	Unknown	1.3%
Silt, with other material	SI3	Unknown	0.8%
Organic material	OR	Unknown	0.7%
Gravel, with traces of fine-grained material	GR3	Unknown	0.5%
Conflicting Aquifer/Aquitard	CONF	Unknown	0.3%
Volcanic rock	VO	Unknown	0.2%
Shell	LL	Unknown	0.1%
Conglomerate	CM	Unknown	0.1%
Shale	SH	Unknown	0.0%

3.3 ACT Modelling

The ACT modelling combines the information from the SkyTEM-derived resistivity models with the lithological classification from boreholes to translate resistivities into clay content (CF model). It results in a data pair of CF-resistivity for each resistivity layer at each model location.

Based on the basic assumption of the HSM-concept (lower electrical resistivity equals lower hydraulic conductivity and vice versa), the CF model is generated based on a translator function defined by two parameters:

- A lower resistivity threshold (m_{low}): resistivity values under will be assigned a CF of 1, meaning they are considered to be close to aquitard conditions.
- An upper resistivity threshold (m_{up}): resistivity values above will be assigned a CF of 0, meaning they are considered to be close to aquifer conditions.

All other resistivity values between m_{low} and m_{up} will get assigned CF values between 0 and 1. Starting values for m_{low} and m_{up} are required to be assigned at the initiation of an ACT model run, and the inversion process adjusts these at every ACT model node to find a best fit to data.

Figure 3.2 represents histograms of the resistivity model values corresponding to pure gravel and pure clay lithologies. Both primary lithology and the full description of the lithological logs were analysed for gravel and clay content, and all resistivities in a 100 m radius of those bore logs were extracted, with depth intervals matched. Based on the histograms, the values of 40 and 100 ohm.m were defined as the optimum starting points for the translator function cutoffs m_{low} and m_{up} (i.e. we expect almost no gravel below 40 ohm.m and almost no clay above 100 ohm.m). Some iterative testing was also undertaken around these values to confirm they are the optimal starting values (i.e. running tests of start value combinations between 30–50 ohm.m and 80–120 ohm.m).

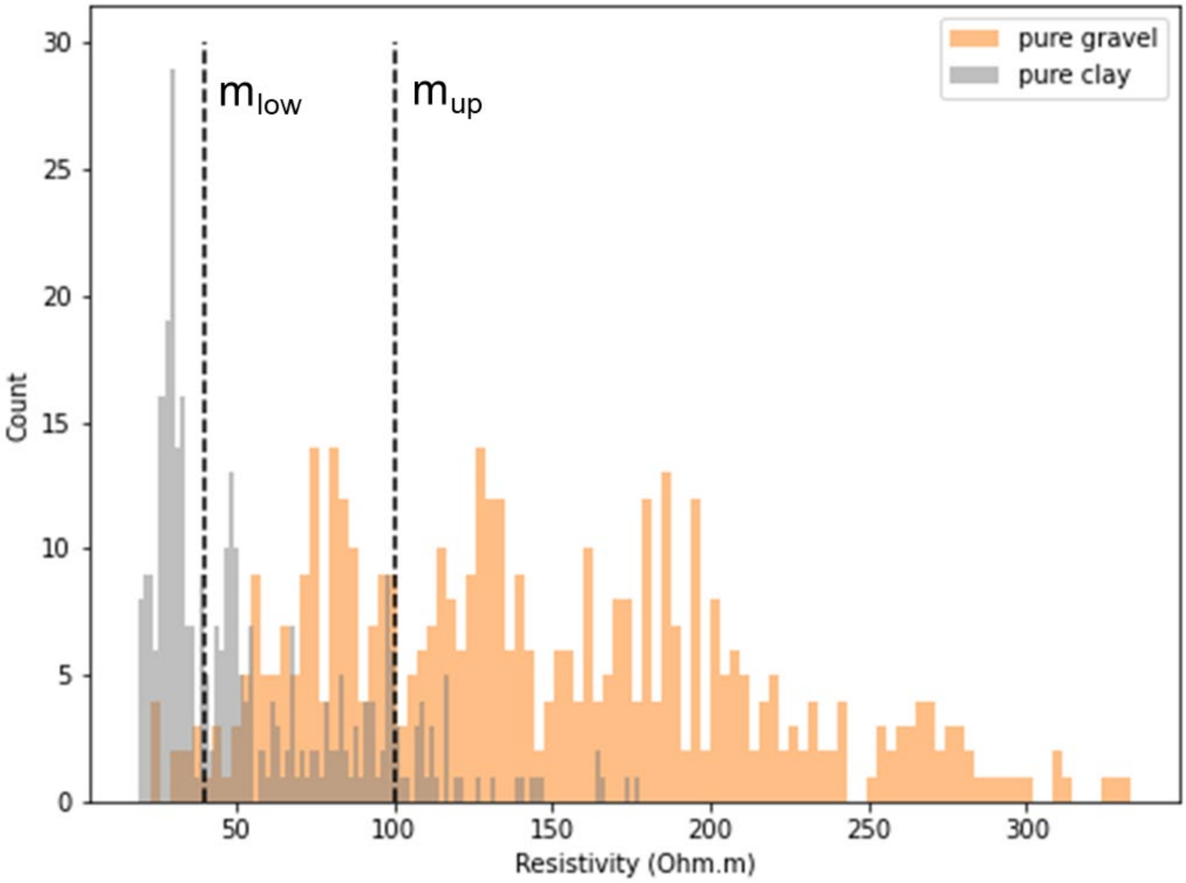

Figure 3.2 Histogram of resistivity values corresponding to pure gravel and pure clay lithology. The dotted lines represent the values chosen as optimum parameters of the translator function start values (m_{low} at 40 ohm.m and m_{up} at 100 ohm.m)

The ACT modelling utilises a 3D grid of translator function nodes. The vertical discretisation of the ACT translator function grid follows the same layering as the input resistivity model, with the exception of the first six layers (upper 8.4 m) grouped into three layers. Due to the resistivity model being clipped by the hydrogeological basement surface, the deepest layer of the model reaches a depth of 234.2 m below ground level, resulting in a 25-layer model. Due to the size of the survey area and limitations in computational power, the ACT modelling was conducted in two areas (Figure 2.1), both with a horizontal node spacing of 800 m.

Lithological log QI were used to assign different uncertainties for the lithological data in the HSM-concept, with the uncertainties defined as follows: uncertainty rating of 10% for QI=1 bore logs, 15% for QI=2 bore logs, 30% for QI=3 bore logs, 50% for QI=4 bore logs and QI=5 bore logs were excluded.

A summary of the ACT modelling set up parameters and the resulting data fit for each model is described in Table 3.2.

Table 3.2 ACT model parameters and results table.

<table>
<tr><th colspan="4">Model Input</th></tr>
<tr><td>Resistivity Model</td><td colspan="3">SkyTEM, sharp SCI inversion result (Rawlinson et al. 2022)</td></tr>
<tr><td>Resistivity Model Clipping</td><td colspan="3">Shallower of ‘Standard DOI’ or ‘Hydrogeological basement surface depth + 30 m’ (Section 3.2.1; Sahoo et al. 2023)</td></tr>
<tr><td>Borehole Dataset</td><td colspan="3">Classified and quality-coded lithological logs (Section 3.2.2; Tschritter et al. 2022)</td></tr>
<tr><th colspan="4">Translator Function</th></tr>
<tr><td>Lower Start Value (ohm.m)</td><td>40</td><td>A Priori (Factor)</td><td>99</td></tr>
<tr><td>Upper Start Value (ohm.m)</td><td>100</td><td>Model Layers</td><td>25</td></tr>
<tr><td>Horizontal Model Constraint (Factor)</td><td>2</td><td>Node Distance (X and Y, m)</td><td>800 x 800</td></tr>
<tr><td>Vertical Model Constraint (Factor)</td><td>2.2</td><td>Search Radius (m)</td><td>500</td></tr>
<tr><th colspan="4">ACT Results</th></tr>
<tr><td colspan="2">Model Name</td><td colspan="2">Data Fit</td></tr>
<tr><td colspan="2">Half North (Figure 2.1)</td><td colspan="2">0.9351</td></tr>
<tr><td colspan="2">Half South (Figure 2.1)</td><td colspan="2">1.1086</td></tr>
</table>

3.4 Clustering

A K-means clustering routine was applied on the ACT results to convert the CF-resistivity data pairs to a number of discrete hydrostratigraphic units. In Aarhus Workbench, the number of clusters chosen is one of the input parameters of the clustering calculation; therefore, to define the optimal number of clusters for this dataset, inertia was computed (Figure 3.3). The ideal result of inertia is both a low inertia and a low number of clusters. To identify this ideal value, the elbow point of the graph was picked (after this point, the improvement in the inertia is not significant).

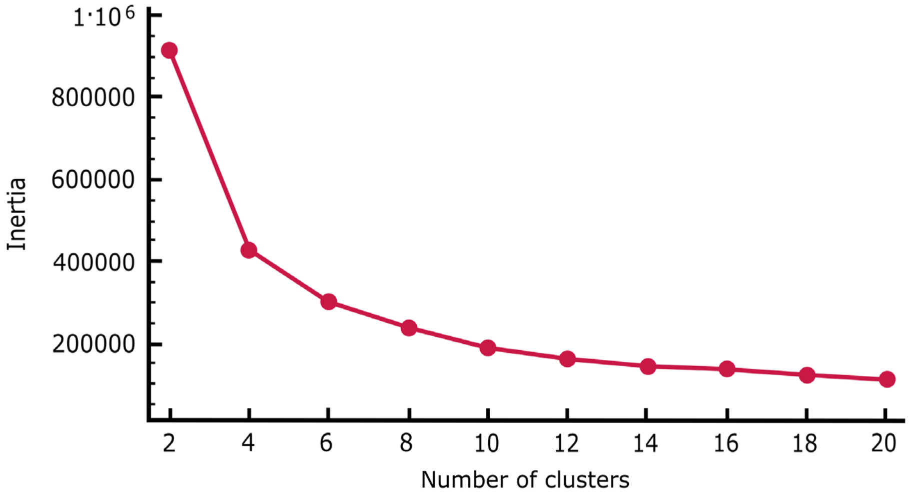

Figure 3.3 Inertia curve. Using the elbow method, the optimal number of clusters for this dataset is 6.

Following the result of the inertia computation, the clustering routine was implemented with six clusters. Cluster 1 corresponds to the least permeable sediments and Cluster 6 to the most permeable sediments (Figure 3.4).

The final step of the HSM-concept implemented in this study was the computation of the silhouette index in Aarhus Workbench (Figure 3.4). The silhouette index is a measure of how similar an object is to its own cluster (cohesion) compared with other clusters (separation). The mean silhouette index for this dataset is 0.55; this value could be used as a threshold value for hard data selection in later hydrological modelling (e.g. Foged 2022).

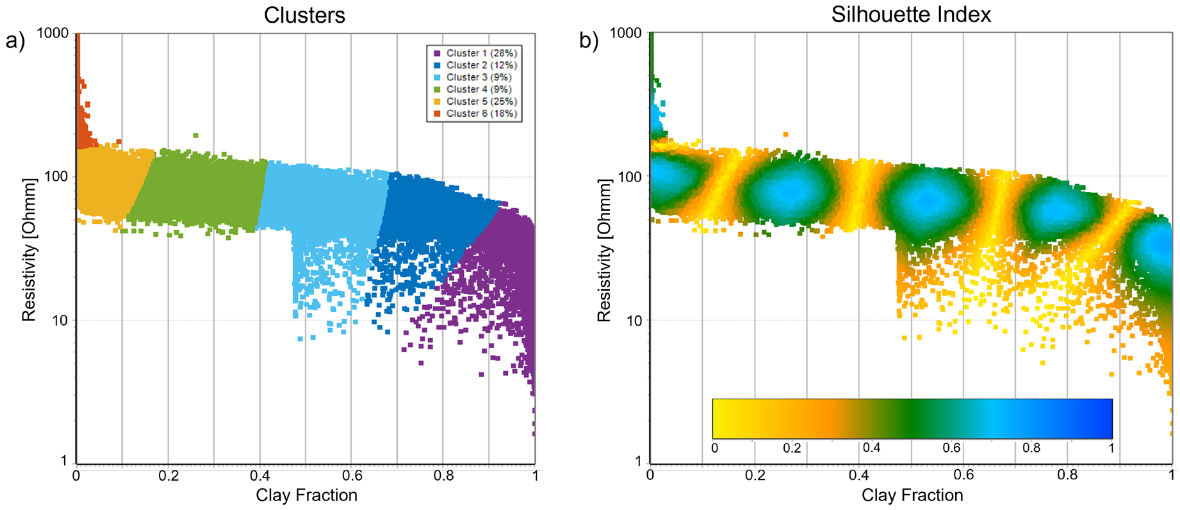

Figure 3.4 Clustering result of the ACT modelling. (a) Input Clay Fraction (x-axis) and resistivity data (y-axis) and the resulting six cluster groups (point colour). Cluster 1 corresponds to the least permeable material (i.e. clay) and Cluster 6 corresponds to the most permeable material (i.e. gravel). (b) Corresponding silhouette index for each cluster. The mean silhouette index is 0.55.

The primary interval-based output file from Aarhus Workbench was converted into csv format for easy accessibility. This file was then converted to a point format for easier interpolation to 3D grids by vertically resampling each interval into five points. Each file contains X and Y coordinates, elevation, resistivity, CF, cluster and silhouette index data.

4.0 RESULTS

Through the iterative testing of the ACT model, boreholes were manually assessed to enable the best data fit possible (Table 3.2). Around 35% of the lithological data enters the ACT modelling classified as “no data”, this reduces the uncertainty of the resulting CF- resistivity data pairs. It is also important to note that there is a dependence on the inherent uncertainty of the bore log descriptions quality (Tschritter et al. 2022).

A cross-section example of the results obtained in the Ruataniwha Plains in the study is provided in Figure 4.1. Here, Cluster 1 is the least permeable material and Cluster 6 is the most permeable material. Clusters 1 and 2 correspond to >0.65 clay fraction; Cluster 3 is a broad transitional group, ranging from 0.4 to 0.7 clay fraction; and Clusters 4–6 correspond to <0.45 clay fraction. Only 9% of the input data fall into the transitional Cluster 3 group (Figure 3.4).

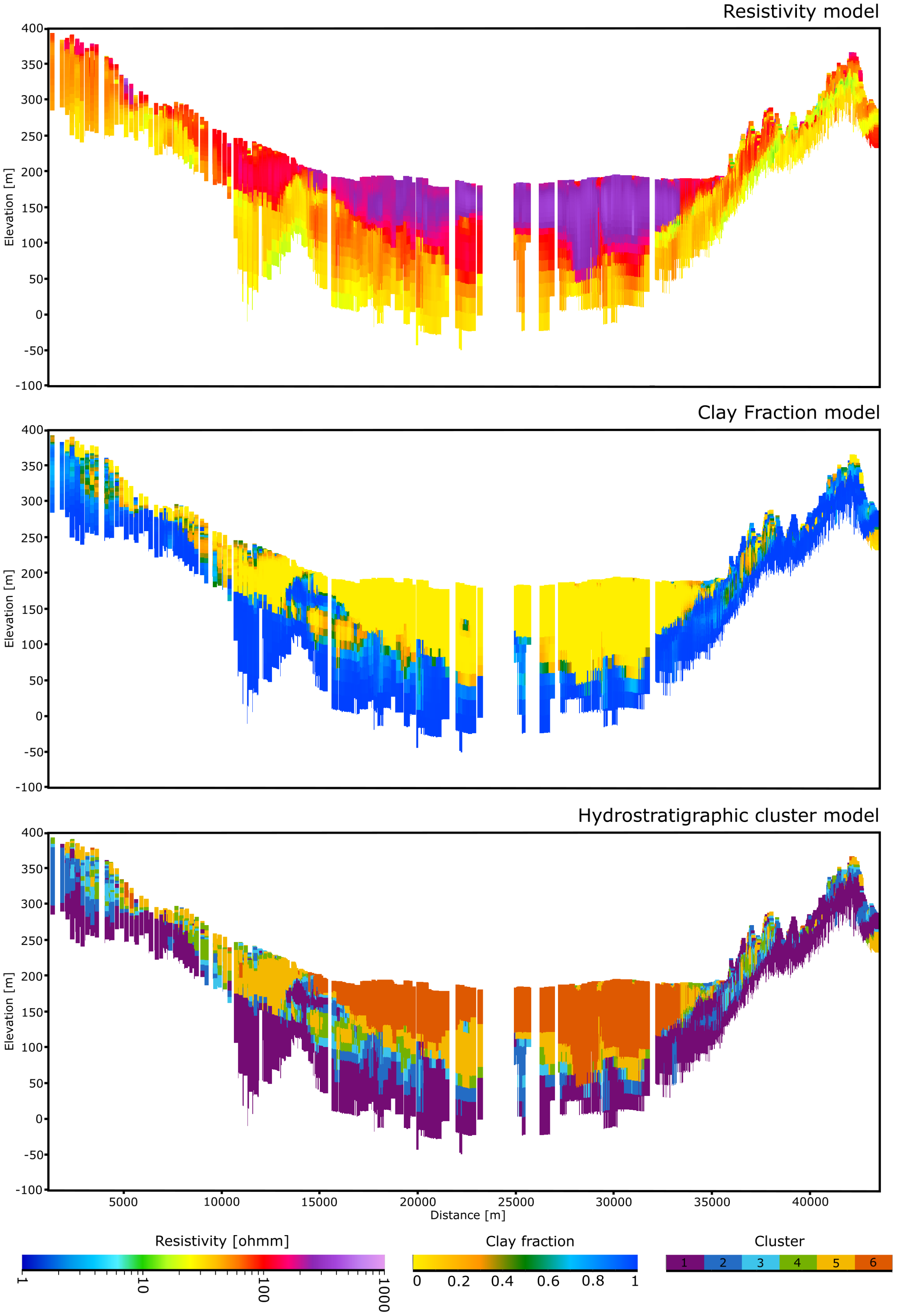

Figure 4.1 Cross-section (location in Figure 2.2) showing from top to bottom, the sharp SkyTEM-derived resistivity model utilised for the ACT modelling, the CF model (~0 = aquifer, ~1 = aquitard) and the hydrostratigraphic cluster model. Cluster 1 represents the most clay rich/least permeable unit and Cluster 6 represents the lowest clay content/most permeable unit.

5.0 DELIVERABLES

All data are geo-referenced to the New Zealand Transverse Mercator (NZTM 2000) spatial reference system.

Descriptions of the formats of the three deliverable files below are provided as a *.docx file: *Ruataniwha_HSM_file_description.docx*

The primary dataset delivered is an interval-based csv file: *Ruataniwha_HSM_2023.csv*

This file was vertically resampled to five points per interval for easier interpolation to 3D grids, and is also provided as an x,y,z *.csv file: *Ruataniwha_Resampled_HSM_2023.csv*

The adapted borehole dataset with the rock symbol classification utilised is also provided as a *.csv file: *Ruataniwha_bores_HSM_2023.csv*

6.0 ACKNOWLEDGEMENTS

This work has been jointly funded by the New Zealand Government's PGF, HBRC and GNS Science's SSIF (Ministry of Business, Innovation and Employment).

Thank you to Nikolaj Foged of TEM Company and Anders Christiansen of Aarhus University HydroGeophysics Group (HGG) for discussions related to this project. Thank you to Amanda Langley of Project Haus for project management support.

Thank you to Chris Worts for business partnerships support. We thank Rob Reeves and Conny Tschritter of GNS Science, as well as Simon Harper and Tom Wilson of HBRC for their review of this report.

Yours sincerely,

Maiwenn Herpe Hydrogeologist	Zara Rawlinson Senior Hydro-Geophysicist

7.0 REFERENCES

Christiansen AV, Foged N, Auken E. 2014. A concept for calculating accumulated clay thickness from borehole lithological logs and resistivity models for nitrate vulnerability assessment. *Journal of Applied Geophysics.* 108:69–77. https://doi.org/10.1016/j.jappgeo.2014.06.010

Foged N, Marker PA, Christansen AV, Bauer-Gottwein P, Jørgensen F, Høyer A-S, Auken E. 2014. Large-scale 3-D modeling by integration of resistivity models and borehole data through inversion. *Hydrology and Earth System Sciences*. 18(11):4349–4362. https://doi.org/10.5194/hess-18-4349-2014

Foged N. 2022. Hawke’s Bay 3D Aquifer Mapping Project: Heretaunga Plains, 3D hydrostratigraphic modelling. Aarhus (DK): Aarhus University HydroGeophysics Group. 27 p. Prepared for Hawke’s Bay Regional Council.

Hemmings B, Moore C, Rawlinson ZJ, Taves M. In prep. Hawke’s Bay 3D Aquifer Mapping Project: Numerical Groundwater Modelling experiments using SkyTEM data in the Heretaunga Plains. Lower Hutt (NZ): GNS Science. Consultancy Report. Prepared for Hawke’s Bay Regional Council.

Marker PA, Foged N, He X, Christiansen AV, Refsgaard JC, Auken E, Bauer-Gottwein P. 2015. Performance evaluation of groundwater model hydrostratigraphy from airborne electromagnetic data and lithological borehole logs. *Hydrology and Earth System Sciences*. 19(9):3875–3890. https://doi.org/10.5194/hess-19-3875-2015

[PDP] Pattle Delamore Partners. 1999. Ruataniwha Plains conceptual hydrogeological model. Napier (NZ): Hawke’s Bay Regional Council. Technical report EMT 99/3.

Rawlinson ZJ. In prep. Hawke’s Bay 3D Aquifer Mapping Project: 3D hydrogeological models from SkyTEM data in the Heretaunga Plains. Wairakei (NZ): GNS Science. Consultancy Report 2023/57. Prepared for Hawke’s Bay Regional Council.

Rawlinson ZJ, Reeves RR, Westerhoff RS, Foged N, Pederson JB, Kellett RL. 2022. Hawke’s Bay 3D Aquifer Mapping Project: Ruataniwha Plains SkyTEM data processing and resistivity models. Wairakei (NZ): GNS Science. 79 p. Consultancy Report 2022/38. Prepared for Hawke’s Bay Regional Council. https://www.hbrc.govt.nz/assets/Document-Library/Reports/Hawkes-Bay-3D-Aquifer-Mapping-project-Ruataniwha-Plains-SkyTEM-data-processing-and-resistivity-models.pdf

Sahoo T, Rawlinson Z, Kellett R. 2023. Hawke’s Bay 3D Aquifer Mapping Project: delineation of hydrogeological basement within the Ruataniwha Plains from SkyTEM-derived resistivity models. Lower Hutt (NZ): GNS Science. 10 p. Consultancy Report 2023/39LR. Prepared for Hawke’s Bay Regional Council.

SkyTEM Australia Pty Ltd. 2020. Acquisition and processing report: SkyTEM helicopter EM survey, Hawkes Bay, NZ. Malaga (AU): SkyTEM Australia Pty Ltd. 33 p. Report AUS 10056. Prepared for Hawke's Bay Regional Council.

Tschritter C, Herpe M, Kellett RL, Rawlinson ZJ, Arnot MJ, Griffin AG, Lawrence MJF. 2022. Hawke’s Bay 3D Aquifer Mapping Project: Ruataniwha Plains data and model inventory. Wairakei (NZ): GNS Science. 111 p. Consultancy Report 2022/76. Prepared for Hawke’s Bay Regional Council. https://www.hbrc.govt.nz/assets/Document-Library/Hawkes-Bay-3D-Aquifer-Mapping-Project-Ruataniwha-Plains-data-and-model-inventory.pdf

Vilhelmsen T, Marker P, Foged N, Wernberg T, Auken E, Christiansen AV, Bauer-Gottwein P, Christensen S, Høyer A-S. 2019. A regional scale hydrostratigraphy generated from geophysical data of varying age, type and quality. *Water Resources Management*. 33(2):539–553. https://doi.org/10.1007/s11269-018-2115-1